Bioorganic & Medicinal Chemistry Letters 22 (2012) 5025–5030

Contents lists available at SciVerse ScienceDirect

Bioorganic & Medicinal Chemistry Letters

journal homepage: www.elsevier.com/locate/bmcl

Design, synthesis, modeling, biological evaluation and photoaffinity labeling studies of novel series of photoreactive benzamide probes for histone deacetylase 2

Aditya Sudheer Vaidya [a,†], Bhargava Karumudi [a,†], Emma Mendonca [b], Antonett Madriaga [a], Hazem Abdelkarim [a], Richard B. van Breemen [a], Pavel A. Petukhov [a,*]

[a] Department of Medicinal Chemistry and Pharmacognosy, College of Pharmacy, University of Illinois at Chicago, 833 South Wood Street, Chicago, IL 60612, USA
[b] Department of Bioengineering, University of Illinois at Chicago, 851 South Morgan Street, Chicago, IL 60607, USA

ARTICLE INFO

Article history:
Received 12 April 2012
Revised 4 June 2012
Accepted 6 June 2012
Available online 18 June 2012

Keywords:
Benzamides
HDAC 1 and 2
Time-dependent inhibition
Photoaffinity labeling
Diazides

ABSTRACT

The design, modeling, synthesis, biological evaluation of a novel series of photoreactive benzamide probes for class I HDAC isoforms is reported. The probes are potent and selective for HDAC1 and 2 and are efficient in crosslinking to HDAC2 as demonstrated by photolabeling experiments. The probes exhibit a time-dependent inhibition of class I HDACs. The inhibitory activities of the probes were influenced by the positioning of the aryl and alkyl azido groups necessary for photocrosslinking and attachment of the biotin tag. The probes inhibited the deacetylation of H4 in MDA-MB-231 cell line, indicating that they are cell permeable and target the nuclear HDACs.

Histone deacetylases (HDACs) are considered viable drug targets for multiple therapeutic applications including cancer and neurological diseases.[1,2] Recently, Cravatt et al.[3] and Gottesfeld et al.[4] described the design and applications of photoaffinity probes for profiling HDACs in native proteomes and live cells. The scaffold of the probes included a portion of a pan HDAC inhibitor suberoyl anilide hydroxamic acid (SAHA), a benzophenone group as a photoreactive group, and an alkyne handle to attach an azide containing reporter tag via (3+2) cycloaddition. Attempts to use the same features based on HDAC1 and 2 selective benzamide scaffolds resulted in probes with HDAC potency above 180 μM in HeLa cell nuclear lysate.[5]

We have already established the Binding (E) nsemble (Pro) filing with (F) photoaffinity (L) abeling approach (BEProFL) where we have experimentally mapped the multiple binding modes of diazide based photoreactive probes for HDACs.[6] The design of these probes included decoration of HDAC ligands with a 3-azido-5-azidomethylene moiety, a photoaffinity labeling group originally proposed by Suzuki et al.[7] for specific labeling of the catalytic portion of HMG-CoA reductase. The aromatic azido moiety was used as a photoreactive group and the aliphatic azide was well suited for (3+2) cycloaddition with an alkyne moiety of the biotin-containing reporter group. Based on these features, we have successfully designed and synthesized highly potent and selective probes for HDAC3 and HDAC8 and demonstrated that they are cell permeable and exhibit excellent antiproliferative activity against several cancer cell lines.[8] Our main objective in this study was to design photoreactive benzamide probes for HDAC2 and evaluate their activity/selectivity profile for other class I HDAC isoforms.

We hypothesized that a set of potent and selective benzamide-based probes capable of crosslinking with HDAC2 can be designed by appropriately decorating benzamides **1** and **2** (Fig. 1) with a combination of the aryl and alkyl azides. Both **1** and **2** and their derivatives were reported by Delorme,[9] Miller,[10] Gangloff,[11] and their colleagues to be active and selective inhibitors of HDACs1 and 2.

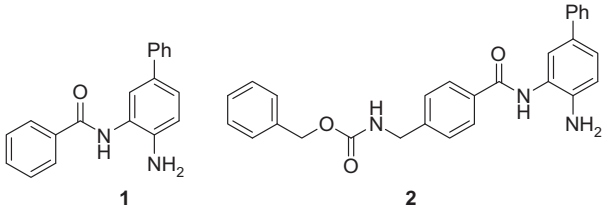

Figure 1. Benzamide inhibitors of HDAC 1 and 2.

* Corresponding author. Tel.: +1 312 996 4174; fax: +1 312 996 7107.
E-mail address: pap4@uic.edu (P.A. Petukhov).
† These authors contributed equally to the work.

0960-894X/$ - see front matter © 2012 Elsevier Ltd. All rights reserved.
http://dx.doi.org/10.1016/j.bmcl.2012.06.017

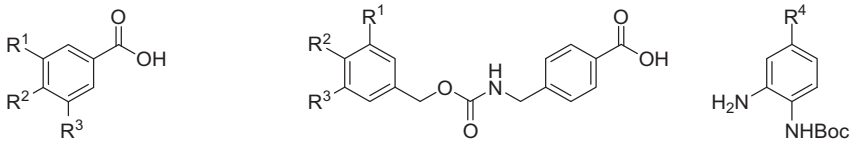

3, R^1 = H, R^2 = N_3, R^3 = H
4, R^1 = N_3, R^2 = H, R^3 = CH_2N_3
5, R^1 = N_3, R^2 = -$O(CH_2)_2N_3$ H, R^3 = H
6, R^1 = H, R^2 = $NHCO(CH_2)_2N_3$, R^3 = H

7, R^1 = N_3, R^2 = H, R^3 = H
8, R^1 = N_3, R^2 = H, R^3 = CH_2N_3

9, R^4 = Ph
10, R^4 = 2-thiophenyl
11, R^4 = N_3

Figure 2. Amine and acid precursors used for synthesis of photoreactive probes.

Substituted benzoic acids **3**–**8**, mono-*N*-Boc protected phenylenediamines **9**, **10** and azidoaniline **11** shown in (Fig. 2) were chosen as precursors for the synthesis of the photoreactive probes. Acid **4**, protected phenylendiamines **9**, **10**, and intermediates **16**, **18** and **19** were synthesized as reported previously,[7,8,10,12] whereas benzoic acid **3** was available commercially. The synthesis of precursors **5**, **6**, **7**, **8**, and **11** is shown in Schemes 1 and 2. The synthesis of the probes **1a**–**g** and **2a**–**b** proceeded through an efficient carbodiimide based coupling reaction between mono-*N*-Boc protected phenylendiamines **9**–**11** and benzoic acids **3**–**8** followed by deprotection of the resulting *N*-Boc products to give the final probes in 70–80% overall yield[13] (Scheme 2).

The inhibitory profile of the probes against class I HDAC isoforms was determined using a fluorogenic assay and the results are given in Table 1. The inhibition of HDAC8 was measured using the fluorogenic acetylated substrate Fluor de Lys and purified recombinant human HDAC8 from *Escherichia coli*,[14] whereas the inhibition of HDAC1–3 was measured using fluorogenic acetylated substrate Boc-L-Lys(Ac)-AMC and commercially available recombinant human HDAC1–3.[15] We also explored the effect of preincubation with HDAC1, 2, 3, and 8 as it was previously observed that the potency of the benzamide-based HDAC inhibitors increased with preincubation with HDAC1–3.[11,16] The maximum incubation time was chosen on the basis of stability of HDAC proteins in the conditions used to determine IC_{50} values. We found that for HDAC1, 3, and 8 the maximum incubation time was 3 h, whereas HDAC2 protein was stable for 24 h. The IC_{50} values of ligands **1** and **2** determined in this study vary from those reported previously.[10,11] We attribute this discrepancy to the differences in the assay conditions, the protein sources, substrates, and preincubation times. The analysis of SAR was facilitated by docking all the probes to HDAC2 (PDB:3MAX),[11] HDAC3 (PDB:4A69),[17] and HDAC8 (PDB:1T69)[18] using GOLD v.5.1.[19,20]

All the newly synthesized benzamide-based probes had activity ranging between 70 nM and 55 μM and 110 nM and 77 μM for HDAC1 and HDAC2, respectively. All of the probes demonstrated a robust 2- to 40-fold increase in inhibition of HDAC1 and 2 upon preincubation with the enzymes for 3 h and 24 h, respectively (Table 2). Consistent with the previously reported observation,[11] SAHA, a hydroxamate-based inhibitor, did not exhibit time-dependent inhibition. Similar trends were observed with HDAC3 and HDAC8. In the discussion below we will use only IC_{50}'s obtained at the maximum preincubation time, unless specified otherwise.

In general, the probes exhibited better activity and selectivity for HDAC1 and 2 as compared to HDAC3 and HDAC8 (Table 1). The most HDAC1 and 2 potent probe **1b** had an estimated 100- and 1000-fold selectivity for HDAC1 and 2 as compared to HDAC3 and HDAC8, respectively. In the case of HDAC8, no inhibition was observed after 5 min, whereas inhibition of HDAC3 varied from 2% for **1g** to 21% for **2c** at 10 μM concentration of the inhibitors. After preincubation for 3 h, inhibition of HDAC3 and HDAC8 by the probes varied from 6.5% for **1g** to 56% for **1b** and from 4.7% for **1b** to 26% for **1g**, respectively. Similarly to the probes, ligand **1** showed pronounced inhibition of HDAC3 and HDAC8, 96% and 24%, respectively, and ligand **2** inhibited 40% of activity of HDAC3 and only 3% of activity of HDAC8. Despite the similarity of probes **2a**–**c**, **2a** did not inhibit HDAC8 at 10 μM, whereas both **2b** and **2c** inhibited 25% and 22% of activity of HDAC8, respectively.

Gangloff et al.[11] suggested that the time-dependent inhibition in the case of HDAC2 may be explained by the gradual disruption of the internal hydrogen bond between the aniline hydrogen and carbonyl oxygen in the unbound form of the ligand so as to form a bidentate complex with Zn^{2+} ion in the bound form. After a preincubation 3 h, increase in inhibition of HDAC1 and HDAC2 by the probes varied from 1.6-fold for **1d** to 17-fold for **1b** and from 1.3-fold for **1g** to 7.1-fold for **2c**, respectively, (Table 2). After

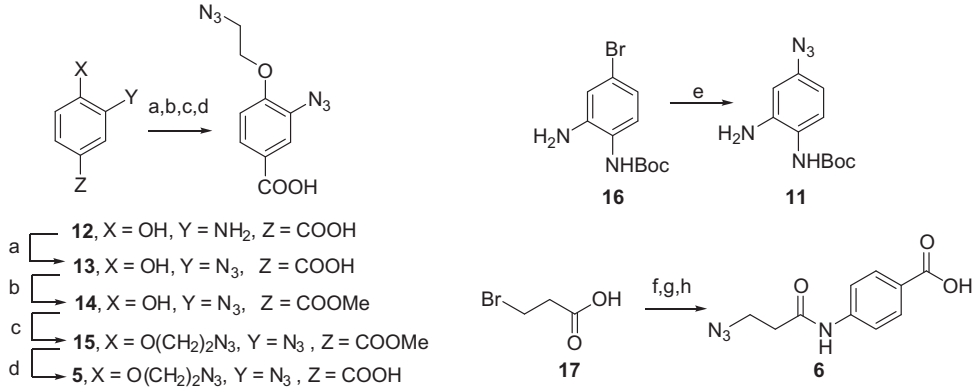

a: **12**, X = OH, Y = NH_2, Z = COOH
b: **13**, X = OH, Y = N_3, Z = COOH
c: **14**, X = OH, Y = N_3, Z = COOMe
d: **15**, X = $O(CH_2)_2N_3$, Y = N_3, Z = COOMe
5, X = $O(CH_2)_2N_3$, Y = N_3, Z = COOH

16 **11** **17** **6**

Scheme 1. Reagents and conditions: (a) $NaNO_2$, HCl, NaN_3, 5 h, 0 °C–rt, 85%; (b) $SOCl_2$, MeOH, 8 h, 0 °C –rt, 87%; (c) K_2CO_3, 2-azidoethyl-4-methylbenzene sulphonate, acetone, 5 h, reflux, 77%; (d) THF/H_2O (1:1), KOH, 10 h, 70 °C, 92%; (e) NaN_3, Sod. ascorbate, CuI, *N*,*N*-dimethylethane-1,2-diamine, EtOH/H_2O, reflux, 92%; (f) (i) NaN_3, CH_3CN, reflux, 80%; (ii) oxalyl chloride, DCM, 6 h; (g) methyl 4-aminobenzoate, pyridine, DCM, 0 °C–rt, 86%; (h) 2 N NaOH, THF/H_2O (8:2), 2 h, rt, 93%.

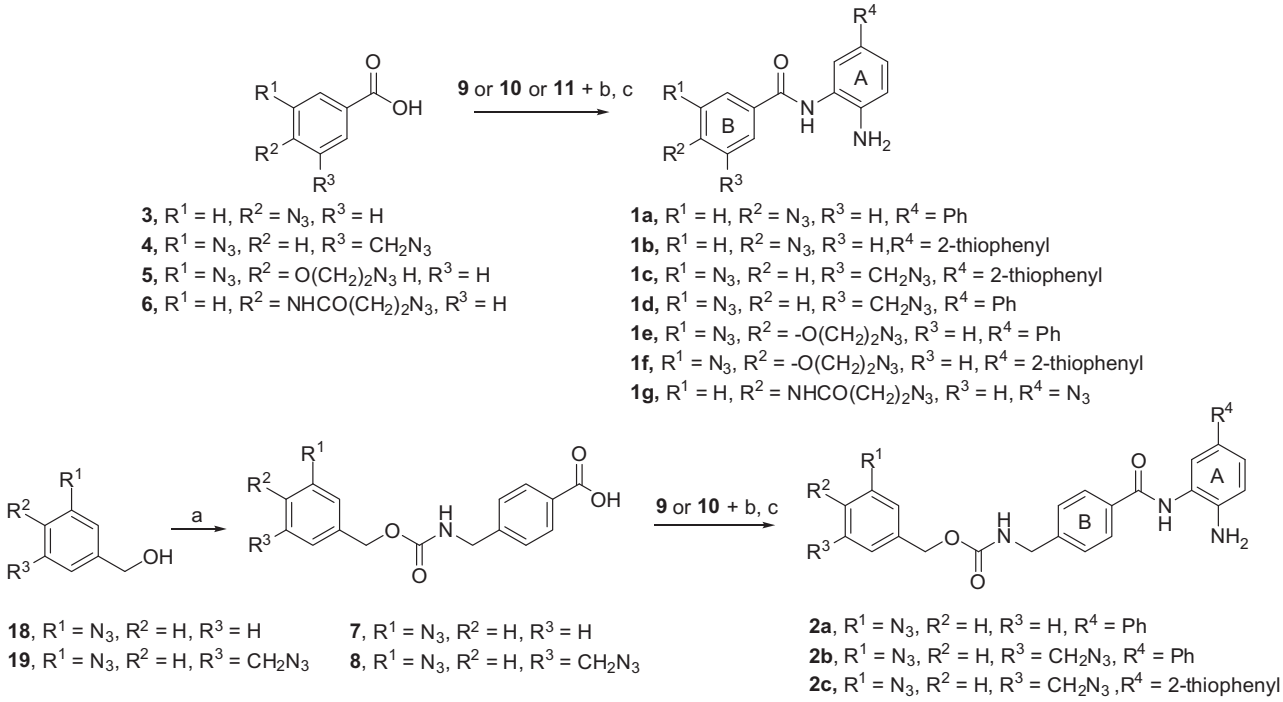

Scheme 2. Reagents and conditions: (a) CDI, DBU, TEA, 4-(aminomethyl)benzoic acid, THF, 10 h, 0 °C–rt, 90–92%; (b) EDCI, HOBt, DMF, 12 h, 80 °C, 80–90%; (c) TFA/DCM, 0.5 h, rt, 90–95%.

Table 1
Potency of the probes against class I HDAC isoforms

#	HDAC1 IC_{50} (nM)		HDAC2 IC_{50} (nM)			HDAC3 % inhibition (10 μM)		HDAC8 % inhibition (10 μM)	
	Preincubation time		Preincubation time			Preincubation time		Preincubation time	
	5 min	3 h	5 min	3 h	24 h	5 min	3 h	5 min	3 h
1a	2100 ± 44	140 ± 34	5130 ± 470	1050 ± 81	210 ± 17	6.6	35	NA	NA
1b	1200 ± 85	70 ± 5.3	3200 ± 260	690 ± 57	110 ± 36	8.7	56	NA	4.7
1c	5600 ± 520	1400 ± 160	18000 ± 910	5200 ± 400	2400 ± 74	2.2	27	NA	11
1d	21000 ± 100	13000 ± 320	32000 ± 1700	21000 ± 720	10000 ± 490	NA	24	NA	14
1e	23000 ± 1400	2700 ± 69	34000 ± 2300	6500 ± 120	830 ± 28	4.3	16	NA	22
1f	18000 ± 130	3800 ± 54	17000 ± 4400	6600 ± 140	750 ± 81	7.6	12	NA	6.6
1g	96000 ± 1600	55000 ± 1300	120000 ± 4900	94000 ± 530	77000 ± 4100	2.0	6.5	NA	26
2a	3800 ± 120	780 ± 22	3800 ± 540	1000 ± 70	320 ± 32	7.8	48	NA	NA
2b	2500 ± 280	990 ± 53	7000 ± 250	1100 ± 25	350 ± 16	11	46	NA	25
2c	2800 ± 240	1210 ± 68	7100 ± 220	1000 ± 50	300 ± 77	21	47	NA	22
1	410 ± 16	52 ± 4.3	1200 ± 93	350 ± 15	140 ± 8	26	96	NA	24
2	14500 ± 1300	1880 ± 5.2	38000 ± 2000	14000 ± 1030	740 ± 49	8.8	40	NA	3.0
SAHA	29 ± 1.6	34 ± 3.2	200 ± 14	ND	260 ± 4.3	100	100	100	100

NA, no inhibition up to 10 μM concentration; ND, not determined. Data are mean ± SD of three independent experiments.

preincubation for 24 h, inhibition of HDAC2 further improved to 1.6-fold for **1g** to 41-fold for **1e**. A comparison of the IC_{50} ratios for 3 h versus 5 min and 24 h versus 5 min for HDAC2 (Table 2) shows that the weakest inhibitors **1c**, **1d**, and **1g** exhibit the least pronounced change in their IC_{50} with time. A somewhat similar but less pronounced trend is observed in the case of HDAC1. In general, the trends observed in our case seem to be consistent with the explanation for the time-dependent inhibition given by Gangloff et al.[11] The difference in the time-dependent inhibition by the probes that have the same substituent binding to the 'foot pocket', for example, **1a**, **1d**, **1e**, **2a**, and **2b**, at 3 h versus 5 min and 24 h versus 5 min suggests that additional factors should be taken into account. Overall ability of the ligands to adopt the necessary conformation for induced fit may play a role in addition to the conformational flexibility of the benzamide portion of the ligands. HDAC1 is highly homologous to HDAC2, and, therefore, its time-dependent inhibition may be explained in a similar fashion. However, neither HDAC3 nor HDAC8 were reported to have crystal structures that would contain a binding pocket similar to the 'foot pocket' of HDAC2. The docking of the probes to HDAC2 showed that their binding poses are essentially the same as that of ligand **1**, that is, the aniline nitrogen and the amide oxygen form a bi-dentate chelate with Zn^{2+}, whereas the bi-aryl portion occupies the 'foot pocket' (Figs. 3 and 4).

A comparison of the docking pose of probe **2c** in HDAC2, HDAC3, and HDAC8 shows that, unlike HDAC2 (Fig. 3A), HDAC3 (Fig. 3B) and HDAC8 (Fig. 3C) cannot accommodate **2c** such that it can form a bi-dentate complex with Zn^{2+} in the catalytic site. The binding site of HDAC3 in 4A69 is too small for **2c** and the probe is mostly resides outside the binding site. In HDAC8 in 1T69, the binding site is too short and has a somewhat different shape compared to HDAC2. None of the docking poses of **2c** coordinates with

Table 2
Ratios of IC_{50} for HDACs 1, 2 and 3 with respect to preincubation time and selectivity for HDAC1 versus 2

#	HDAC1 IC_{50} ratio 3 h/5 min	HDAC2 IC_{50} ratio 3 h/5 min	HDAC2 IC_{50} ratio 24 h/5 min	HDAC3 %inhibition ratio 3 h/5 min	HDAC2/HDAC1 IC_{50} ratio 3 h/3 h	HDAC2/HDAC1 IC_{50} ratio 24 h/3 h
1a	15	4.9	24	5.3	7.5	1.5
1b	17	4.6	29	6.4	9.9	1.6
1c	4.0	3.5	7.5	12	3.7	1.7
1d	1.6	1.5	3.2	–	1.6	0.77
1e	8.5	5.2	41	3.7	2.4	0.31
1f	4.7	2.6	23	1.6	1.7	0.20
1g	1.7	1.3	1.6	3.3	1.7	1.4
2a	4.9	3.8	12	6.2	1.3	0.41
2b	2.5	6.4	20	4.2	1.1	0.35
2c	2.3	7.1	24	2.2	0.82	0.25
1	7.9	3.4	8.6	3.7	6.7	2.7
2	7.8	2.7	52	4.5	7.5	0.39
SAHA	0.85	ND	0.77	1.0	ND	7.7

ND, not determined.

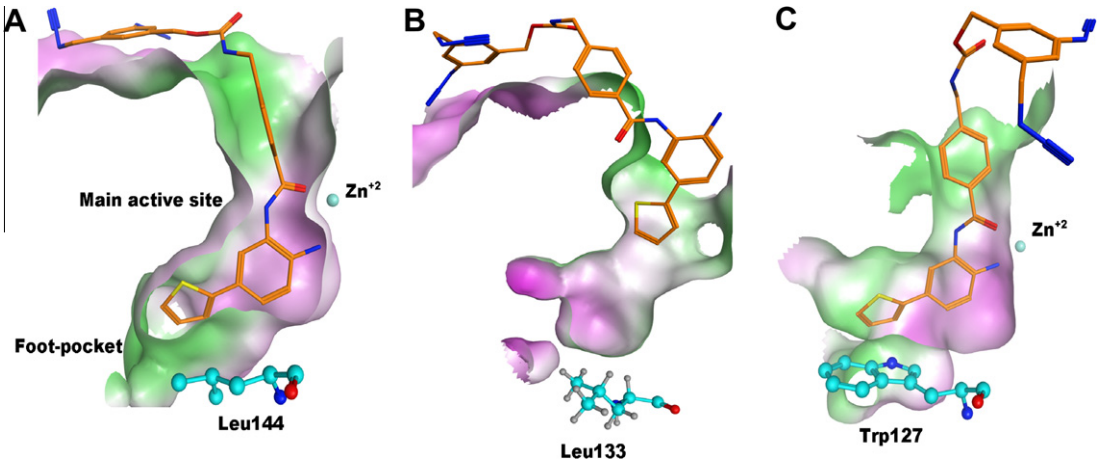

Figure 3. Probe **2c** docked into the active site of (A) HDAC2, (B) HDAC3, and (C) HDAC8.

Zn^{2+} despite the proximity of the groups necessary for coordination. After a co-minimization of **2c** with the HDAC8, only coordination between the carbonyl oxygen of **2c** and Zn^{2+} was observed. Interestingly, although the residues in the foot pocket of HDAC2 and the corresponding residues in HDAC3 (according to sequence alignment) are the same, the recent X-ray apo-structure of HDAC3[17] did not contain a 'foot pocket'. Schwabe et al.[17] noted that the HDAC3 structure was crystallized in the absence of the ligand and, therefore, may not be representative of the actual protein–ligand complex interactions. In our opinion, the similarity of the time-dependent inhibition of HDAC2 and HDAC3 and HDAC8 suggests that the latter two isoforms may also adopt the conformation with a 'foot pocket' that can accommodate the benzamide-based ligands. The relatively low inhibition of HDAC8 compared to HDAC1-3 may be rationalized by the difference in the residues at the entrance to the 'foot-pocket' that imposes different steric and electrostatic requirements on the R^4 substituent. In HDAC8, the opening to the putative 'foot pocket' is hindered by the presence of bulky sidechain of Trp127 as shown in Fig. 3, whereas in HDAC1, 2 and 3 the corresponding residue Leu144 is less bulky and more flexible and makes the 'foot pocket' more accessible to the ligands. This is also indirectly supported by the SAR—probe **1g** is consistently the least active against HDAC1–3 but its inhibition of HDAC8 is comparable to that of **1**, **1e**, **2b**, and **2c**.

Cravatt et al.[5] attributed the low potency of benzophenone based benzamide probes to the positioning of the photoreactive group. Based on their observations, we decided to carry out a small SAR study to explore how the positioning of the aryl azide and aliphatic azide affects the potency and selectivity of the probes. Despite the presence of additional azido groups, probes **1a** and **1b** were comparable in potency to ligand **1** and probes **2a**–**c** were more than 2- to 2.5-fold more potent than ligand **2** for HDAC1 and 2. Probes **1c**–**g** were 27- to 1000- and 5- to 550-fold less potent than ligand **1** for HDAC1 and 2, respectively. In general, probes **1a**–**g** were found to be less potent than ligand **1** for both HDAC3 and 8, whereas compounds **2a**–**c** and ligand **2** demonstrated comparable potency against HDAC3. In HDAC8, the diazide probes **2b** and **2c** appear to be more potent than ligand **2** and the monoazide probe **2a** was inactive. To gain insights into the plausible explanations for the difference in potency we compared the docking poses of the probes with that of ligand **1**. We observed that the *meta*-substituents R^1 and R^3 are too close to the residues Phe210, Gly154, Phe155, Leu276, and Asp104 (Fig. 4).

As a result of this steric interference, the probes are forced to adopt a conformation where the face-to-face π–π stacking between ring B of the probes and Phe155 is disrupted. The loss of these π–π stacking interactions may explain relatively poor potency of mono *meta*-substituted probes **1e** and **1f**, 830 and 750 nM, respectively, and especially 3,5-disubstituted probes **1c** and **1d**, 2.4 and 10 μM, respectively, compared to probes with no *meta*-substituents **1a** and **1b**, 210 and 110 nM, respectively. The width and shape of the gorge region appears to be important to gain potency and isoform selectivity as demonstrated by Kozikowski et al.[21] in design of tubastatin A, a selective inhibitor of HDAC6.

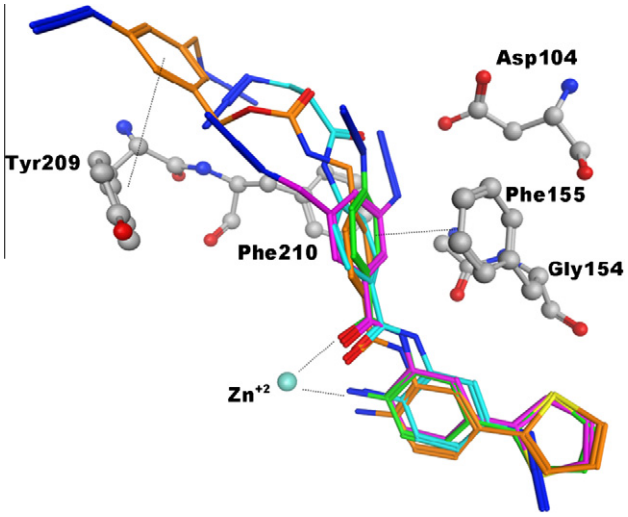

Figure 4. Overlay of compounds **1b** (green), **1c** (magenta), **1g** (cyan) and **2c** (gold) in the active site of HDAC2.

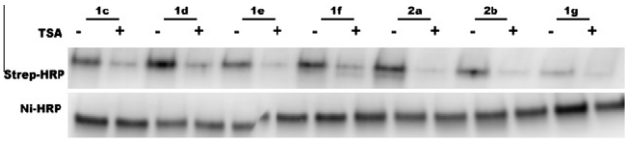

Figure 5. Characterization of biotinylated HDAC2 and His-tagged HDAC2 using streptavidin-HRP and nickel-HRP. Western blot analysis of diazide probes **1c**, **1d**, **1e**, **1f**, **2b**, **2c** and **1g** (25 μM) photocrosslinked to HDAC 2 (1.25 μM) in the presence or absence of 125 μM of Trichostatin A using streptavidin-HRP and nickel-HRP. Shown is the representative western blot of three independent experiments.

Placement of the aromatic azido group in the 'foot-pocket' in **1g** led to poor potency for HDAC1 and 2, 55 and 77 μM, respectively, slightly less pronounced decrease in inhibition of HDAC3 but not HDAC8. The docking showed that the R^4 azido substituent fits well in the 'foot pocket' and occupies the same space as the R^4 phenyl and 2-thiophenyl substituents in **1a**–**f**. This observation appears to be consistent with the SAR found by Methot et al.,[22] where non-polar aromatic substituents were found to be preferable compared to polar and/or relatively small substituents R^4. The additional interactions between the carbamate appendage in probes **2a**, **2b** and **2c** and Tyr209 of HDAC2 identified by docking did not contribute to potency of these ligands, suggesting that this appendage is likely to remain solvent exposed.

Next we investigated whether the newly designed probes are capable of crosslinking HDAC2. Photoaffinity labeling studies were conducted with the probes using commercially available recombinant His-tagged HDAC2. The probes (25 μM) were preincubated with HDAC2 (1.25 μM) for 24 h in photolabeling buffer, exposed to 254 nm UV light for 3 × 1 min with 1 min resting. A commercially available strained cyclooctyne based biotin tag (BT) was attached to the HDAC2-probe adduct using (3+2) cycloaddition reaction and the biotinylated HDAC2 was visualized by streptavidin-HRP and western blot analysis (Fig. 5). The loading was confirmed by using nickel-HRP, which recognized the His-tag of the recombinant HDAC2 protein.[23] To ensure that the biotinylation was primarily driven through interactions of the probes with the binding site of HDAC2, we performed competition experiments of the probes with a known potent HDAC inhibitor Trichostatin A (125 μM), which has an IC_{50} of 68 nM for HDAC2. [8] All of the diazide probes showed a pronounced decrease in biotinylation in the presence of five-fold molar excess of the competing ligand. The decrease was slightly less pronounced in the case of weakly potent probe **1g**.

We also confirmed that our probes **1a**–**f** and **2a**–**c** are cell permeable and capable of inhibiting nuclear HDACs by monitoring the acetylation status of histone H4 in MDA-MB-231 breast cancer cell line using previously published procedure.[24] H4 is a known nuclear target for HDAC1 and HDAC2 in this cell line.[25] All of the probes inhibited deacetylation of histone H4 at 50 μM concentration after a 24 h treatment (Fig. 6A and B).

In conclusion, two benzamide scaffolds were successfully explored for design of novel HDAC2 nanomolar potent and selective photoreactive probes suitable for further BEProFL experiments. A total of 10 monoazide and diazide containing benzamide probes were synthesized and tested for their inhibitory activity against class I HDAC isoforms. All the probes are readily accessible in few synthetic steps carried out in a convergent manner. The inhibition was measured at two time points for HDAC1, 3, and 8 and three points for HDAC2. The probes exhibited a 2- to 40-fold increase in inhibition with respect to time for HDAC1 and 2 and modest increase was observed for HDAC3 and 8. Time-dependent inhibition of HDAC1, 3, and 8 suggests that these isoforms may also adopt the 'foot pocket' conformation similar to that of HDAC2 to accommodate the benzamide ligands. The most potent probes exhibit nanomolar activity against HDAC1 and 2. Probe **1b** has an IC_{50} of 70 and 110 nM for HDAC1 and 2, respectively, and shows an estimated 100- to 1000-fold selectivity for HDAC1 and 2 as compared to HDAC3 and 8. The most active diazide probes **2b** and **2c** have an IC_{50} of 0.9 and 1.2 μM and 300 and 350 nM for HDAC1 and 2, respectively, and show approximately 30-fold selectivity for HDAC1 and 2 as compared to HDAC3 and 8. Docking studies with HDAC2 indicated that the placement of the azido groups meta

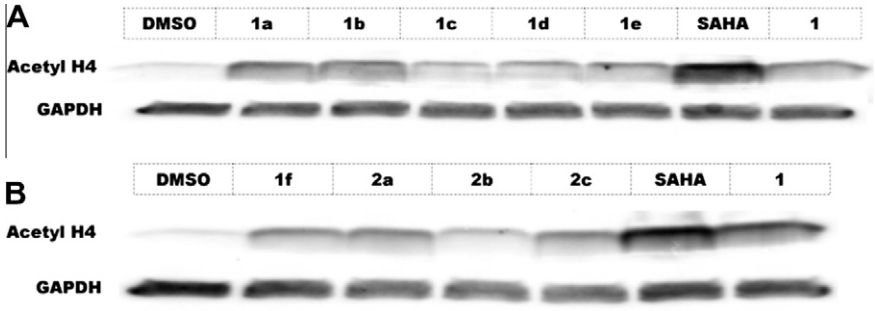

Figure 6. Western blot detection of acetyl H4 in MDA-MB-231 cell lines following a 24 h treatment with probes at 50 μM. (A) Treatment of cells with probes **1a**, **1b**, **1c**, **1d**, **1e**, suberoyl anilide hydroxamic acid (SAHA) and parent ligand **1**. (B) Treatment of cells with probes **1f**, **2a**, **2b**, **2c**, suberoyl anilide hydroxamic acid (SAHA) and parent ligand **1**. Shown is a representative blot of three independent experiments.

but not *para* to the benzamide group in ring B leads to unfavorable for π–π stacking between ring B and Phe155 orientation of the ligand. Consistent with earlier reports, the presence of the bi-aryl moiety in the 'foot-pocket' was found to be essential for maintaining potency for HDAC1–3. On the other hand, **1g**, a probe that lacks the bi-aryl portion found in **1a**–**f** and **2a**–**c**, was found to be superior to the bi-aryl-containing probes in inhibiting of HDAC8. As demonstrated by our photolabeling experiments, all the diazide probes efficiently photocrosslinked with recombinant HDAC2. Cell based studies show that the benzamide probes are able to enter the cell nucleus and trigger accumulation of acetylated H4. Presently, the probes are being extensively used in mapping the binding site of HDAC2 via proteomics experiments. Cell based photolabeling experiments are currently underway to understand how these probes bind to HDAC complexes in cells.

Acknowledgments

This study was funded by the National Cancer Institute/NIH Grant R01CA131970 and ADDF Grant #20101103. We thank Professor Carol Fierke, University of Michigan, MI, for generously providing us with the plasmid for in-house expression and purification of HDAC8.

References and notes

1. Khan, O.; La Thangue, N. B. *Immunol. Cell Biol.* **2012**, *90*, 85.
2. Mai, A.; Rotili, D.; Valente, S.; Kazantsev, A. G. *Curr. Pharm. Des.* **2009**, *15*, 3940.
3. Salisbury, C. M.; Cravatt, B. F. *Proc. Natl. Acad. Sci. U.S.A.* **2007**, *104*, 1171.
4. Xu, C.; Soragni, E.; Chou, C. J.; Herman, D.; Plasterer, H. L.; Rusche, J. R.; Gottesfeld, J. M. *Chem. Biol.* **2009**, *16*, 980.
5. Salisbury, C. M.; Cravatt, B. F. *J. Am. Chem. Soc.* **2008**, *130*, 2184.
6. He, B.; Velaparthi, S.; Pieffet, G.; Pennington, C.; Mahesh, A.; Holzle, D. L.; Brunsteiner, M.; van Breemen, R.; Blond, S. Y.; Petukhov, P. A. *J. Med. Chem.* **2009**, *52*, 7003.
7. Hosoya, T.; Hiramatsu, T.; Ikemoto, T.; Nakanishi, M.; Aoyama, H.; Hosoya, A.; Iwata, T.; Maruyama, K.; Endo, M.; Suzuki, M. *Org. Biomol. Chem.* **2004**, *2*, 637.
8. Neelarapu, R.; Holzle, D. L.; Velaparthi, S.; Bai, H.; Brunsteiner, M.; Blond, S. Y.; Petukhov, P. A. *J. Med. Chem.* **2011**, *54*, 4350.
9. Paquin, I.; Raeppel, S.; Leit, S.; Gaudette, F.; Zhou, N.; Moradei, O.; Saavedra, O.; Bernstein, N.; Raeppel, F.; Bouchain, G.; Frechette, S.; Woo, S. H.; Vaisburg, A.; Fournel, M.; Kalita, A.; Robert, M. F.; Lu, A.; Trachy-Bourget, M. C.; Yan, P. T.; Liu, J.; Rahil, J.; MacLeod, A. R.; Besterman, J. M.; Li, Z.; Delorme, D. *Bioorg. Med. Chem. Lett.* **2008**, *10*, 1067.
10. Witter, D. J.; Harrington, P.; Wilson, K. J.; Chenard, M.; Fleming, J. C.; Haines, B.; Kral, A. M.; Secrist, J. P.; Miller, T. A. *Bioorg. Med. Chem. Lett.* **2008**, *18*, 726.
11. Bressi, J. C.; Jennings, A. J.; Skene, R.; Wu, Y.; Melkus, R.; De Jong, R.; O'Connell, S.; Grimshaw, C. E.; Navre, M.; Gangloff, A. R. *Bioorg. Med. Chem. Lett.* **2010**, *20*, 3142.
12. Umezawa, N.; Matsumoto, N.; Iwama, S.; Kato, N.; Higuchi, T. *Bioorg. Med. Chem.* **2010**, *18*, 6340.
13. *General procedure for synthesis of the probes*: To a solution of substituted benzoic acid **3–8** (1.1 equiv) in anhydrous DMF (5 mL/mmol of amine) was added EDCI (1.2 equiv) followed by HOBt (1.2 equiv) and stirred at room temperature for 1 h. Thereafter protected phenylendiamine **9–11** (1 equiv) was added and the mixture heated at 78 °C overnight. After completion of the reaction as confirmed by TLC, saturated sodium bicarbonate solution (20 mL/mmoL of amine) was added and the mixture was extracted with ethylacetate (30 mL/mmol of amine). The organic layer was washed with water (30 mL/mmol of amine), dried over anhydrous sodium sulphate and evaporated in vacuo. The residue was purified using flash chromatography (silica gel, hexane/ethylacetate gradient) to yield the *N*-Boc protected probes. The Boc group was subsequently removed by treating *N*-Boc protected compound with a mixture of TFA/DCM (1:1 v/v) at room temperature for 1 h. The solvent was removed in vacuo and the residue purified using flash chromatography (silica gel, hexane/ethylacetate gradient) to yield the final probes as solids in 70–80% over all yield. Spectral data for probe **1b**; ^{1}H NMR (400 MHz, DMSO-d_6) δ (ppm) 9.83 (bs, 1H), 8.05 (d, J = 8.4 Hz, 2H), 7.40–7.25 (m, 6H), 7.06–7.04 (m, 1H), 6.86 (d, J = 8.4 Hz, 1H). ^{13}C NMR (100 MHz, DMSO-d_6) δ (ppm). 164.13, 144.42, 143.13, 142.33, 131.33, 130.28(2C), 128.75, 124.49, 124.44, 124.36, 123.96, 123.60, 121.80, 119.36(2C), 117.48. (M+H)$^+$ 336.40. Spectral data for probe **2c**; ^{1}H NMR (400 MHz, DMSO-d_6) δ (ppm) 9.79 (bs, 1H), 8.00–7.95 (m, 2H), 7.65–7.55 (m, 3H), 7.52–7.35 (m, 4H), 7.33–7.23 (m, 1H), 7.18 (s, 1H), 7.09 (s, 1H), 6.89 (d, J = 8.4 Hz, 1H), 5.08 (s, 2H), 4.49 (s, 2H) 4.29 (s, 2H). ^{13}C NMR (100 MHz, DMSO-d_6) δ (ppm) 165.39, 156.32, 143.35, 140.15, 140.05 140.01, 138.18 138.16, 133.17, 128.89 (2C), 128.74 (2C), 127.95 (2C), 126.81 (2C), 126.19, 125.61, 124.78, 123.91, 118.24, 117.61, 116.95, 64.46, 52.96, 43.68. (M+H)$^+$ 553.60.
14. Dowling, D. P.; Gattis, S. G.; Fierke, C. A.; Christianson, D. W. *Biochemistry* **2010**, *49*, 5048.
15. HDAC inhibition assay was performed in 96-well opaque half-area microplate (Corning). Human recombinant HDAC1,2 and 3 (BPS Bioscience) and HDAC8 (purified from *E. Coli*) were diluted with assay buffer 1 (25 mM Tris–HCl, pH 8.0, 137 mM NaCl, 2.7 mM KCl, 1 mM $MgCl_2$, and 1 mg/mL BSA), so as to have 4, 5 and 1 ng/μl and 8.5 ng/μL stocks of each isoform, respectively. Serial dilutions of the probes were made in assay buffer 2 (25 mM Tris–HCl, pH 8.0, 137 mM NaCl, 2.7 mM KCl, 1 mM $MgCl_2$). Ten microlitre of the enzyme stock was added to 30 μL of the probes and preincubated for different preincubation times. It was observed the *Z*-factor for the assays remained above 0.7 up to 3 h for HDAC1, 3 and 8 and up to 24 h for HDAC2, hence these preincubation times were chosen for the assays. After preincubation, 10 μL of 125 μM HDAC fluorescent substrate Boc-L-Lys (Ac)-AMC (Chem-Impex) in case of HDAC1,2 and 3 and 10 μL of 25 μM BML-KI-178 (Biomol Inc.) in case of HDAC8 was added, and the mixture incubated for 35 min (HDAC1, 3, 8), 60 min (HDAC2) at room temperature. The reaction was quenched with 50 μL of 1 mg/mL trypsin and 5 μM trichostatin A in assay buffer 1 (25 mM Tris–HCl, pH 8.0, 137 mM NaCl, 2.7 mM KCl, 1 mM MgCl2) and further incubated at room temperature for 35 min. The plate was read on Synergy 4 hybrid microplate reader (BioTeck) at excitation wavelength 360 nm and emission wavelength 460 nm. The IC_{50} values were determined using the GraphPad Prism 5 software (GraphPad Software Inc., La Jolla, CA).
16. Chou, C. J.; Herman, D.; Gottesfeld, J. M. *J. Biol. Chem.* **2008**, *283*, 35402.
17. Watson, P. J.; Fairall, L.; Santos, G. M.; Schwabe, J. W. *Nature* **2012**, *481*, 335.
18. Somoza, J. R.; Skene, R. J.; Katz, B. A.; Mol, C.; Ho, J. D.; Jennings, A. J.; Luong, C.; Arvai, A.; Buggy, J. J.; Chi, E.; Tang, J.; Sang, B. C.; Verner, E.; Wynands, R.; Leahy, E. M.; Dougan, D. R.; Snell, G.; Navre, M.; Knuth, M. W.; Swanson, R. V.; McRee, D. E.; Tari, L. W. *Structure* **2004**, *12*, 1325.
19. Jones, G.; Willett, P.; Glen, R. C.; Leach, A. R.; Taylor, R. *J. Mol. Biol.* **1997**, *267*, 727.
20. Verdonk, M. L.; Cole, J. C.; Hartshorn, M. J.; Murray, C. W.; Taylor, R. D. *Proteins* **2003**, *52*, 609.
21. Butler, K. V.; Kalin, J.; Brochier, C.; Vistoli, G.; Langley, B.; Kozikowski, A. P. *J. Am. Chem. Soc.* **2010**, *132*, 10842.
22. Methot, J. L.; Chakravarty, P. K.; Chenard, M.; Close, J.; Cruz, J. C.; Dahlberg, W. K.; Fleming, J.; Hamblett, C. L.; Hamill, J. E.; Harrington, P.; Harsch, A.; Heidebrecht, R.; Hughes, B.; Jung, J.; Kenific, C. M.; Kral, A. M.; Meinke, P. T.; Middleton, R. E.; Ozerova, N.; Sloman, D. L.; Stanton, M. G.; Szewczak, A. A.; Tyagarajan, S.; Witter, D. J.; Secrist, J. P.; Miller, T. A. *Bioorg. Med. Chem. Lett.* **2008**, *18*, 973.
23. Diazide probe (25 μM) or probe-TSA (25 μM-probe and 125 μM-TSA) mixture was incubated with HDAC2 (1.25 μM) for 24 h in photolabelling buffer (25 mM Tris–HCl, pH 8.0, 137 mM NaCl, 2.7 mM KCl, 1 mM $MgCl_2$, 0.1% Triton-X), exposed to 254 nm UV light 3 × 1 min with 1 min resting. A solution of 500 μm of DBCO-PEG4-biotin conjugate (Click Chemistry tools) in photolabeling buffer was added to initiate the (3+2) cycloaddition reaction with HDAC2-probe adduct. The cycloaddition reaction was carried out for 3 h at room temperature. Western blotting was done with 1.5 μg of purified protein with 5× loading buffer containing 10% SDS, 0.05% bromophenol blue, 50% glycerol, and β-mercaptoethanol. Protein samples were boiled for 5 min and allowed to cool before loading on a denaturing 4–15% polyacrylamide gel electrophoresis (SDS–PAGE). After electrophoresis, protein was transferred to a polyvinylidiene difluoride membrane (Iblot-Invitrogen). The membrane was incubated for 12 h with 5% albumin fraction V (Sigma–Aldrich) in 1× Tris based saline supplemented with 0.1% Tween-20 (TBST). The membrane was washed three times with TBST and then incubated with Ni-HRP (1:2000) in TBST for 1 h under room temperature with slight agitation. After three washes in TBST, the chemilumiscent signal was detected using the enhanced chemiluminescence (ECL) kit from Pierce (Pierce Biotechnology, Rockford, IL). The membrane was washed three times with 1 × phosphate buffer saline supplemented 0.1% Tween-20 (PBST), and stripped of Ni-HRP by incubating with 5% BSA, 2 M Imidazole in PBST for 1 h at room temperature. After three washes of PBST, the membrane was incubated with Streptavidin-HRP (1:5000) in PBST for 1 h. After three washes in PBST and water, the chemilumiscent signal was detected using the enhanced chemiluminescence (ECL) kit from Pierce (Pierce Biotechnology, Rockford, IL).
24. MDA-MB-231 cells seeded at 1.0 × 10^5 cells/well in 6-plates and grown to 90% confluence in DMEM (Gibco) supplemented with 10% FBS (Gibco) and 1% penicillin-streptomycin (Mediatech). Cells were treated with either DMSO or benzamide probes at a final concentration of 50 μM and maintained at 37 °C and 5% CO_2 for 24 h. Cells were lysed using 1 × RIPA buffer (150 mM NaCl, 1% Triton X-100, 0.5% sodium deoxycholate, 0.1% SDS, 50 mM Tris, pH 8.0) containing protease inhibitor cocktail (Roche) and 1:100 dilution of phosphatase inhibitor (Sigma) with shearing. Lysates were clarified through centrifugation at 13,000 rpm at 4 °C. Total protein concentration was determined via the BCA Protein Assay Kit (Pierce). Lysates were stored at −20 °C until later use. Sample vials were prepared by aliquoting 25 μg of total protein and adding 5× Sample buffer. Sample vials were boiled for 5 min, cooled to RT, and proteins separated by gel electrophoresis at 80 V. Proteins in the gel were transferred to PVDF membrane in 4 min using the Invitrogen iBlot system. Membranes were blocked using 5% Milk in PBST and probed using anti-GAPDH (1:5000) or anti-acetyl histone H4 (1:1000) overnight at 4 °C. Membranes were incubated with either anti-mouse (1:5000) or anti-rabbit (1:5000) in 5% Milk in PBST. Results were visualized using Femto chemiluminescent substrate (Pierce) in CCD camera.
25. Suzuki, J.; Chen, Y. Y.; Scott, G. K.; Devries, S.; Chin, K.; Benz, C. C.; Waldman, F. M.; Hwang, E. S. *Clin. Cancer Res.* **2009**, *15*, 3163.